Developments in the Built Environment 16 (2023) 100228

Contents lists available at ScienceDirect

Developments in the Built Environment

journal homepage: www.sciencedirect.com/journal/developments-in-the-built-environment

Investigation of thermophysical properties of Turkey oak particleboard for sustainable building envelopes

Rupali Tiwari [a,b,*], Vlastimil Boháč [b], Roman Réh [a], Valentina Lo Giudice [c], Luigi Todaro [c], Viliam Vretenár [b], Vladimír Štofanik [b], Lubos Kristak [a]

[a] Faculty of Wood Sciences and Technology, Technical University in Zvolen, T. G. Masaryka 24, 96001, Zvolen, Slovakia
[b] Institute of Physics, Slovak Academy of Sciences (IP SAS), Dúbravská Cesta 9, 84511, Bratislava, Slovakia
[c] School of Agricultural, Forestry, Food and Environmental Sciences, University of Basilicata, Viale dell'Ateneo Lucano 10, 85100, Potenza, Italy

ARTICLE INFO

Keywords:
Oak medium density particleboard (MDPB)
Oak high density particleboard (HDPB)
Pulse transient method (PTM)
Uncertainty analysis and sensitivity coefficients

ABSTRACT

The article investigates the thermophysical parameters of Turkey oak particleboard with different densities and their response to varying heat pulse power to cover possible thermally dependent disturbance effects during the measurement. Samples were measured by the Pulse Transient Method using a Cuboid Model to estimate all basic thermophysical parameters. The aim was to assess the properties of the two different particleboard of high and medium density and compare them with published data. We also calculated uncertainties based on sensitivity coefficients analysis for the cuboid model. This methodology helps to assess how the input error propagates into the resulting parameter estimate and helps to optimize the experiment. The quality of oak particleboard holds significant importance in building construction. Additionally, the analysis results assess the suitability of different materials for improving energy efficiency in building construction. Interestingly even slight density differences and thickness can significantly impact the effectiveness of building insulation properties of materials.

1. Introduction

Wood is widely used as a construction material with thermal insulation properties in various industries and housing, including construction, furniture manufacturing, cladding, house insulation, energy-saving houses, and general wood working. *Quercus cerris* L. tree also known as Turkey oak, belongs to the *Fagaceae* family of flowering plants, which is incorporated by beech or oaks. This category of plants includes several tree genera, encompassing *Quercus* (oaks), *Fagus* (beeches), and *Castanea* (chestnuts). This tree spreads from southeastern Europe and its territory includes countries such as Turkey, Greece, Italy, Romania, and Bulgaria. It is not native to Central Europe, but it does occur. In terms of energy conservation, turkey oak is considered the best type of tree due to its foliage and it is well suited to environments with seasonal changes and can withstand harsh climatic conditions. The length of turkey oak can reach up to 25–40 m. The aesthetic appeal of turkey oak with gray bark makes it popular for indoor living and outdoor landscaping.

Various classes of particleboard are used quite widely in the construction industry as a good cladding material with relatively good thermal insulation properties (Ghobadi and Sepasgozar, 2023). The Turkey oak particleboard has impressive thermal conductivity, high heat capacity, and inherent fire resistance. This makes them an excellent choice for construction purposes (Taib et al., 2022). In addition, their durability and sustainability make them a greener option compared to materials such as plastic and metal, as they play an important role in the natural ecosystem (Darwish and Eldeeb, 2023). Turkey oak particleboard have been shown to offer excellent thermal protection, especially for wall or floor coverings. As a sustainable process, oak particleboard is generally made from recycled wood particles and sawdust combined with formaldehyde-based adhesives (Hua et al., 2022). Unfortunately, formaldehyde is a volatile organic compound responsible for releasing harmful gases into the environment or into the home. (Kristak et al., 2023).

Moreover, to address this issue researchers are actively engaged in manufacturing formaldehyde-free binders for particleboard (Akinyemi et al., 2019; Solt et al., 2019; Essid et al., 2021). Therefore, the use of

* Corresponding author. Faculty of Wood Sciences and Technology, Technical University in Zvolen, T. G. Masaryka 24, 96001, Zvolen, Slovakia.
E-mail addresses: tiwari@tuzvo.sk, rupali.tiwari@savba.sk (R. Tiwari), vlastimil.bohac@savba.sk (V. Boháč), reh@tuzvo.sk (R. Réh), logiudicevalentina2@gmail.com (V. Lo Giudice), luigi.todaro@unibas.it (L. Todaro), viliam.vretenar@savba.sk (V. Vretenár), vladimir.stofanik@savba.sk (V. Štofanik), kristak@tuzvo.sk (L. Kristak).

https://doi.org/10.1016/j.dibe.2023.100228
Received 7 July 2023; Received in revised form 28 August 2023; Accepted 6 September 2023
Available online 7 September 2023

these particleboards can be beneficial to the environment and contribute to renewable energy programs. It is very crucial to select the particleboard with low or no formaldehyde emission and optimize the efficiency of building envelopes. It is also important to understand the behavior and interaction of heat with particleboard. Knowledge of thermal conductivity and thermal resistance allows builders and designers access to its thermal insulating properties.

Classifying wood-based composite materials as a high, medium, or low-density board is a misnomer and confusing in general terms because the final manufactured panel of the same density made from light and hard wood particles used in fiber or particles form is different. It is always necessary to accurately characterize the material that has been subjected to research. In our case, we prepared two particleboard sample sets classified as medium density (768.89 kg m^{-3}) and high density (838.65 kg m^{-3}). It is not clear to which class those samples belong as in the published data those data range in different ways. Medium density particleboard (MDPB) comes typically with a density of 680 kg m^{-3} to 730 kg m^{-3} and High density particleboard (HDPB) which are stronger and harder have a typical density of up to 900 kg m^3 (EUROTECH Vacuum Technologies). This classification is not unified and the border between them ranges from 730 up to 800 kg m^{-3}. Youjie Xu published that the density range for medium density particleboard is within 590 ÷ 800 kg m^{-3} (Xu and Wang, 2019).

Wood is an anisotropic and hygroscopic material, so it is very difficult to summarize the general dependence or relationship between the thermophysical parameters and the factors that influenced the results (Mvondo et al., 2020; Lagüela et al., 2015a).

Several advanced techniques are available to measure thermal conductivity, thermal diffusivity, specific heat capacity (Asdrubali et al., 2017), and heat transfer coefficients (Schiavoni et al., 2016). There are two main classes of thermophysical measurement methods. They are divided into stationary or steady state and transient methods. Stationary methods are usually capable of measuring only one parameter. Transient methods measure all three basic thermophysical parameters. The group of established most popular steady state methods, that have the highest accuracy of measuring thermal conductivity, include methods such as the guard hot plate method (Ji et al., 2014; Reddy and Jayachandran, 2017), and the heat flow meter (Yang et al., 2019). Transient or unsteady methods are based on the generation of a heat pulse that causes a dynamic change of the thermal field in the sample and simultaneously records the thermal response to this generated heat at the location of the heat source or a part of it. The temperature distribution in the sample is stabilized and independent of time and space.

$$\frac{dT}{dx} = 0; \ \frac{dT}{dt} = 0$$

The most common transient methods (Yang et al., 2022) used for thermophysical measurements are the PTM (Kubičár et al., 2001; Boháč and Kubičár, 2001), Dynamic plane source technique (hot disk) (Gustafsson, 1991), Extended dynamic plane source technique (EDPS) (Karawacki et al., 1992), Laser flash method (Taoukil et al., 2013) and Hot wire method (Faouel et al., 2012). The thermal response to a small thermal disturbance inside the sample generated by the heat source in the form of a thermal pulse is recorded and Thermophysical parameters are calculated according to the model used. In practice, a heat pulse is created by passing an electric current through a metal resistance in the form of a ball, wire, strip, or plane composed of meander strips. The pulse and stepwise transient methods use a heat pulse generated in the form of a Dirac pulse or a Heaviside step (Kubičár et al., 1999). The thermal response to a heat pulse is recorded by a thermocouple located at a precisely defined distance from the heat source. In this case, the thermal load on the specimen is low and tends to be below 1 °C, so the data obtained corresponds to the thermodynamic state in the real world. This is why transient methods require significantly less measurement time compared to steady-state techniques. They also heat the sample much less, so its structure remains in almost the same thermodynamic state. When performing the experiment, one must pay attention to the correct geometry of the sample, especially in the case of a limited sample size. It is important to plane the sample surface, polish it, and carefully arrange the components of the sample set (Figs. 1 and 3).

In the past decades, research on Turkey oak has increased tremendously. The Turkey oak has shown excellent thermal properties, which has led to greater interest and involvement from researchers and industries alike. The values of the thermal diffusivity κ, thermal conductivity λ, specific heat capacity c, and density ρ of oak were measured using various methods.

Data measured on oriented oak OSB and bulk oak wood under different directions was published by (Kotoulek et al., 2018). The thermal conductivity of oak in the radial direction was 0.133 W.(m.K)$^{-1}$, in the tangential direction 0.112 W.(m.K)$^{-1}$, and in the axial direction 0.262 W.(m.K)$^{-1}$. The thermal conductivity of OSB with a thickness of 10 mm was 0.109 W.(m.K)$^{-1}$ and with a thickness of 15 mm 0.129 W.(m.K)$^{-1}$. The density values of the oak wood samples were in the range of 435.7 ÷ 459.5 kg m^{-3}, whereas the OSB samples were in the range of (411.8 ÷ 418.2) kg m^{-3} (Kotoulek et al., 2018). The densities of these materials were lower than in our experiment but the values of thermal conductivity were similar to our Oak MDPB (0.14 W.(m.K)$^{-1}$).

Çavuş, V. et al. (2019), published measurements of thermal conductivity of different wood materials. The thermal conductivity of Oak (*Quercus petraea* Liebl.) with density 841 kg m^{-3} was 0.917 W.(m.K)$^{-1}$ (min. 0.172 and max. 0.224 W.(m.K)$^{-1}$). Another type of oak wood was white oak (Quercus alba) with a density of 603 kg m^{-3} and a thermal conductivity of 0.148 W.(m.K)$^{-1}$ (min. 0.172 and max. 0.156 W.(m.K)$^{-1}$). All measurements were done on the batch of 15 samples but the angular direction to the grains was not clear for oak wood. They have also discovered the linear relation between thermal conductivity and density. The measurements were performed using THERM 2227–2, ALHBORN meters (Çavuş et al., 2019).

F. Yapici et al. (2011) (Yapici et al., 2011) measured the thermal conductivity of oak (*Quercus robur* L.) in two directions using the Hot-Wire method (ASTM C 1113–99). The thermal conductivity value for parallel and perpendicular orientation to the grain angle had a negligible difference. The thermal conductivity values were 0.2614 W.(m.K)$^{-1}$ for the parallel direction of the grain angle and 0.2584 W.(m.K)$^{-1}$ for the perpendicular direction (Yapici et al., 2011).

In the article Slováčková et al. (2021) (Slováčková, 2021) they study the effect of the wood degradation by Trametes versicolor fungus on the change of thermal conductivity value. The focus of this work was to compare the thermal conductivity values of degraded wood species to reference data of thermal conductivity values of undegraded wood species. The density of the degraded oak heartwood samples was 523.8 kg m^{-3} and the thickness of the sample was 7.78 mm. Degraded oak heartwood had similar λ values as undegraded oak wood. The thermal conductivity values were 0.35 W.(m.K)$^{-1}$ in the longitudinal, 0.20 W.(m.K)$^{-1}$ in the radial, and 0.14 W.(m.K)$^{-1}$ in the tangential direction, whereas the measured values of thermal diffusivity were 4.81 × 10^{-7} m^2 s^{-1} in the longitudinal, 2.65 × 10−7 m^2 s^{-1} in the radial and 2.46 × 10^{-7} m^2 s^{-1} in the tangential direction. The specific heat capacity was 1.32 kJ.(kg.K)$^{-1}$ (Slováčková, 2021). The authors of this article concluded that it is necessary to jointly study the effect of density and moisture content on the values of thermal diffusion, thermal conductivity, and specific heat capacity. It cannot be stated without considering the state of the material structure.

Božiková, M. et al. (2021) (Božiková et al., 2021) performed an experiment on different wood samples as well as on oriented strand board (OSB) made of the same series of different wood, including oak. Samples were measured in the tangential and in the radial direction for thermal diffusivity, thermal conductivity, and volume specific heat parameters. For every wood species the samples were prepared in two directions, the tangential direction (perpendicular to the grain but tangent to the growth rings) and the radial direction (normal to the growth rings). Authors detected relationships between the thermal

Fig. 1. Photo of the High-Density Particleboard (HDPB) (left) and Medium Density Particleboard (MDPB) (right) sample sets. (© V.Boháč, IP SAS).

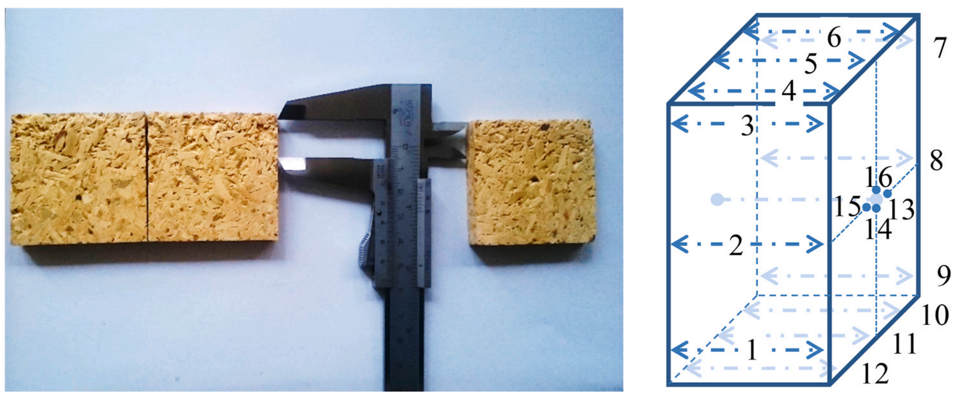

Fig. 2. The sample set on the left and the schematic diagram of the sample part showing all the points used for measuring the thickness dimensions is shown on the right.

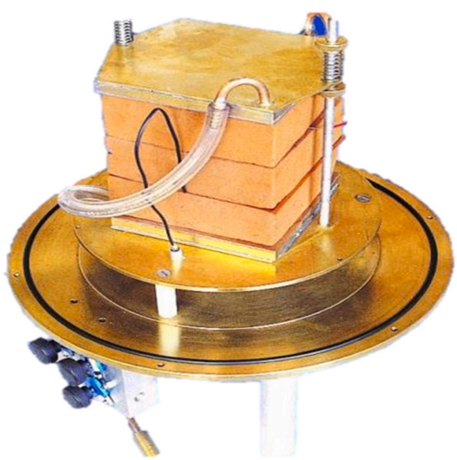

Fig. 3. The RTB 1.02 thermostat chamber, the device includes copper plates as heat exchangers that establish the sample temperature stability (https://fu.sav.sk/veda-a-vyskum/infrastruktura/termofyzikalne-laboratorium/).

parameters in the tangential and the radial direction. The value of thermal conductivity of oak wood in the radial direction was 0.134 W. (m.K) $^{-1}$ and in the tangential direction 0.1164 W. (m.K) $^{-1}$. The value for thermal conductivity of oak wood OSB in the radial direction was 0.156 W. (m.K) $^{-1}$ and 0.139 W. (m.K) $^{-1}$ in the tangential direction. The thermal diffusivity for oak OSB in the tangential and in the radial direction were 0.161 mm^2 s^{-1} and 0.164 mm^2 s^{-1} respectively. The value for volume specific heat was found to be 865 (J.m^{-3}.K^{-1}) in tangential and 951 (J.m^{-3}.K^{-1}) in the radial direction (Table 4 in Božiková et al., 2021). Thermal conductivity in both directions for OSB was higher than for oak wood.

The hygrothermal properties of oak wood with a density of 580.7 kg m^{-3} and porosity of 0.613 were measured in three directions by Jianhua Zhao et al. (2023) (Zhao et al., 2023). Their wood samples had an orthonormal structure, and the moisture properties of oak were measured in three structural directions. The specimens were prepared and cut in the longitudinal direction, tangential direction, and in the radial direction. Moisture or heat transport in wood is a three-dimensional process and occurs simultaneously in all structural directions but at different rates. The ratio of thermal conductivity in the longitudinal direction (0.166 W.(m.K)$^{-1}$) to the radial direction (0.143 W.(m.K)$^{-1}$) and the ratio of thermal conductivity in the longitudinal direction to the tangential direction (0.129 W.(m.K)$^{-1}$) for oak were 1.16 and 1.29 respectively (Zhao et al., 2023). The specific heat capacity of this oak sample was 1171 J.(kg.K)$^{-1}$ (Zhao et al., 2023). Similar behavior was observed for the diffusion of moisture. The water vapor diffusion resistance factor was much smaller in the longitudinal direction due to the longitudinal tracheid cells acting as the main vapor transport pass. Longitudinal absorption of water along tracheid cells and vessels along the stem is always faster than radial and tangential absorption (Zhao et al., 2023).

The article written by S. Lagüela et al. (2015) (Lagüela et al., 2015b) included the measurements of the thermal diffusivity and conductivity of Italian oak, spruce, and larch wood. The Hot Disk method was used to capture thermal conductivity and thermal diffusivity in the longitudinal direction parallel to the grain, whereas radial and tangential directions were measured in the direction of the annual accretion rings (Lagüela et al., 2015b). The dry density of oak wood was determined to be 753.16 kg.m^{-3} and porosity 0.50. According to the configuration of the samples, authors referred to in-plane thermal diffusivity as radial thermal diffusivity, whereas in-depth thermal diffusivity as axial thermal diffusivity. The axial thermal conductivity of oak corresponding to the longitudinal direction was 0.58 W. (m.K) $^{-1}$ and radial conductivity and diffusivity were 0.16 W. (m.K) $^{-1}$ and 1.8 × .10 $^{-7}$ m^2 s^{-1}. The values for tangential direction were 0.21 W. (m.K) $^{-1}$ for axial conductivity and 0.26 W. (m.K)

$^{-1}$ for radial conductivity and $2.82 \times .10^{-7}$ $m^2 s^{-1}$ for radial diffusivity. Finally, for the radial direction, the axial and radial conductivity values were (0.22 and 0.27) W. (m.K) $^{-1}$ and the radial diffusivity $2.91 \times .10^{-7}$ $m^2 s^{-1}$. Since the Hot Disk does not allow the calculation of all unknown parameters for anisotropic materials, the specific heat was measured independently by the DSC method. The value of specific heat capacity measured by DSC was 1214 J.(kg.K)$^{-1}$. The hypothesis from this paper confirmed that the thermal conductivity and diffusivity in the longitudinal direction exceed the values in the radial direction. The principle is that the heat spreads along the wood effortlessly compared to its lateral direction. However, this relative correlation appears to show significant fluctuations influenced by factors such as wood species and moisture content.

1.1. Sample preparation

Turkey oak was supplied by the Meridiana Legnami Company based in Tito Scalo (Potenza). Both types of biomass material were delivered in the form of debarked chips with dimensions of approximately 5 cm in length and varying thickness. The chips were stored in the laboratory for air drying to a moisture content (MC) of approx. 12% for 60 days and then ground into particles using a multifunctional silage crusher with a production efficiency of $\geq$800 kg h^{-1}. The resulting particles were then sieved with horizontal vibrating sieves (Standard Test Method for Particle Size Distribution [ASTM] E−11 Specification) with 4 mm mesh sizes to remove oversize and 0.8 mm to remove dust. Turkey oak MDPB and HDPB were made using 2% urea-formaldehyde (UF) plus 15% modified starch (MS).

The fraction of particles that passed the 4 mm sieve and remained on the 0.8 mm sieve was selected to produce homogeneous single-layer particleboard. The particles ranged in length from 3 to 10 mm, width from 0.5 to 1.5 mm, and thickness from 0.3 to 1 mm. The length, thickness, and width of randomly selected particles (about 30 particles) were measured with a micrometer.

1.2. Measurement setup description

We used the Pulse Transient Method (PTM) for the experimental measurement of thermophysical parameters. Its advantage is that it can be used to determine all basic thermophysical quantities, i.e. thermal conductivity, thermal diffusivity, and specific heat capacity. Moreover depending on the theoretical model used, it is possible to study few more thermal parameters such as the heat transfer coefficient in-between the heat source and the sample, the heat capacity of the heat source, or the heat transfer coefficient from the free surface of the sample to the surroundings in the radial or lateral direction (Boháč et al., 2011, 2023; Tiwari et al., 2021).

This research was motivated by previous results measured on a high-density particleboard made of oak wood chips published in a conference paper (Boháč et al., 2023). In the current work, we used a model for the geometry of a cuboid with a square base to estimate the thermophysical parameters. Using the Levenberg-Marquardt algorithm, we fitted the thermal response measured by PTM in an minimization iterative procedure.

We prepared two sets of oak particleboard samples with high and medium density (HDPB and MDPB) for the measurement. Each set consisted of three parts as shown in Fig. 2. The sample sets were cut in cuboidal geometry with a thickness in the range of $h = 8 \div 9$ mm. The size of sample's square base was 50 mm × 50 mm. The basic sample size was small, and therefore it was necessary to use a cuboid model to account heat losses form the free surface of the sample (Boháč et al., 2011). When measuring thermally low conductive materials, the scanning time of the thermal response is long, while there is a high probability of the influence of heat losses from the surface of the free side of the sample to the surroundings. The thickness of the sample was statistically measured with a caliper at 16 different points (Fig. 2, right) (Tiwari et al., 2021).

The density of the samples was determined by the gravimetric method from the dimensions of the samples and a simple calculation. Moisture content was determined using gravimetric analysis in accordance with ISO 13061–2014 (https://www.iso.org/standard/60063.html). The data of mechanical properties of Turkey oak particleboard are the following for MOE(MPa), MOR(MPa), IB(N. mm^{-2}) (unpublished data):

Oak HDPB: 3590.4 (MOE), 9.0(MOR), 0.6(IB);
Oak MDPB: 3669.9(MOE), 8.1(MOR), 0.55(IB).

To measure the thermophysical parameters of HDPB and MDPB, the experiment required an electronic unit RT-Lab (Štofanik et al., 2007) developed at Institute of Physics, SAS, and a measuring chamber RTB 1.02 (© IP SAS) where the sample was placed between two heat exchanger plates. Plates were stabilized by a thermostat (upper and lower copper plates in Fig. 3).

The entire setup contains various components, for example, the RT-Lab electronic unit controlling measurement, data collection, and data transfer to a computer via USB and TCP/IP port (Štofanik et al., 2007). Another component, the LAUDA thermostat, sets and stabilizes the temperature with an accuracy of ±0.02 K. The RT-Lab electronic unit includes a programmable constant current source to generate the heat pulse, A/D converters to measure the thermal response from the thermocouple, and to measure the background temperature using a PT100 probe. A plane heat source (© IP SAS) was used to generate the heat pulse. It was etched in the shape of a meander from 7 μm thick nickel foil with dimensions of 50 × 50 mm, the total thickness 70 μm and the electrical resistance was 1.7 Ω. (Boháč and Kubičár, 2001). Typical parameters for a thermal response scan are $T_m \sim$ 1K (maximum of thermal response) and t_m (time recorded at T_m). The thermal response is measured using a differential thermocouple of K-type (Chromel-Alumel - diameter 7 μm). By passing the current through this heat source, a heat pulse is generated and thermal response is registered by thermocouple. An experimental arrangement is drawn in Fig. 4.

2. Methodology

The thermophysical properties of Turkey oak particleboard were experimentally measured. The thermal diffusivity, thermal conductivity, and specific heat capacity were measured by the Pulse transient method using different powers of the heat pulse.

In the first step, the thermal response curves were studied for the different powers of the heat pulse generated by different magnitudes of current and different durations of the heat pulse. The thermal responses measured at different pulse powers for MDPB and HDPB were fitted using the cuboid model and compared with each other (Fig. 5 and 6). Thermal response curves varied due to different thicknesses, densities, and heat pulse power levels. The range of pulse energies was obtained by combining the values of the current and the duration of the heat pulse. The basic idea of this part of the experiment was to show the consequences of the quality of the fit using the cuboid model in relation to the experimental data. If the influence of disturbances occurs during the experiment, then a difference occurs, which we usually display in the form of a differential graph (Boháč et al., 2023). If the graph on the time axis shows only the thermal noise of the thermocouple around zero, then we can declare that our model is valid during the time of measuring the thermal response. At a deviation from zero average, usually in the form of a sinusoidal curve, the model ceases to be valid and the data are estimated with a consistent error.

The second step involved investigating the dependence of the thermal response parameters on the power of the heat pulse, as well as the possible correlation between the sensitivity coefficients of thermophysical parameters.

In the third step, all results of estimated thermophysical parameters of MDPB and HDPB were summarized.

The last step was focused on the study of the theory of uncertainty analysis and sensitivity coefficients of the cuboid model which were

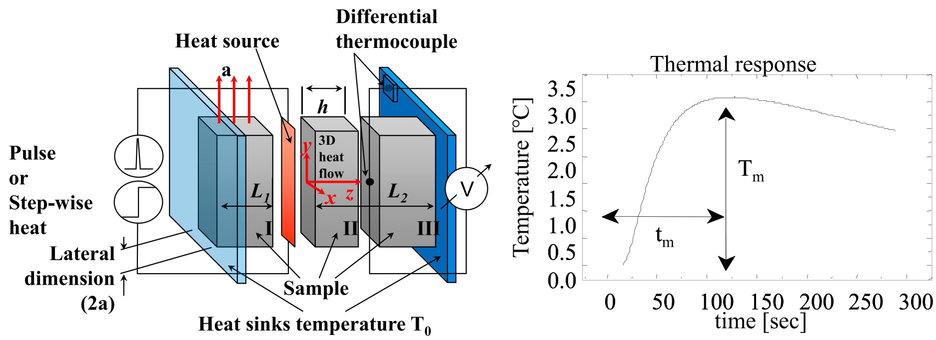

Fig. 4. Experimental setup of the Pulse transient method for cuboid model (left) and example of the thermal response, T_m and t_m are parameters for one point evaluation procedure (right) (Boháč et al., 2023).

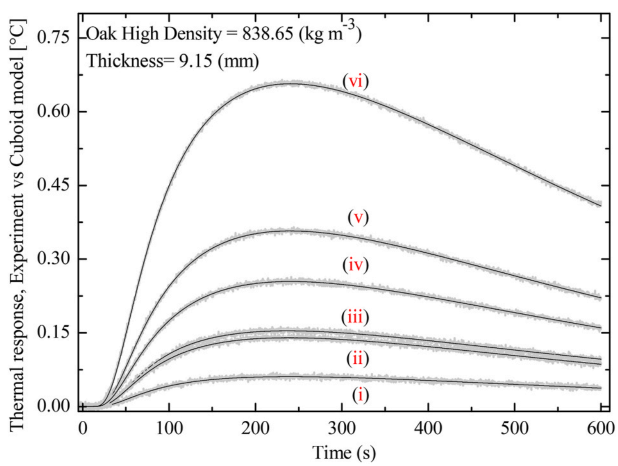

Fig. 5. The experimentally measured (gray) and theoretically calculated (dark black) thermal response curves of Oak HDPB with time duration 600 s are given for different powers of the heat pulse (density 838.65 kg m^{-3}).

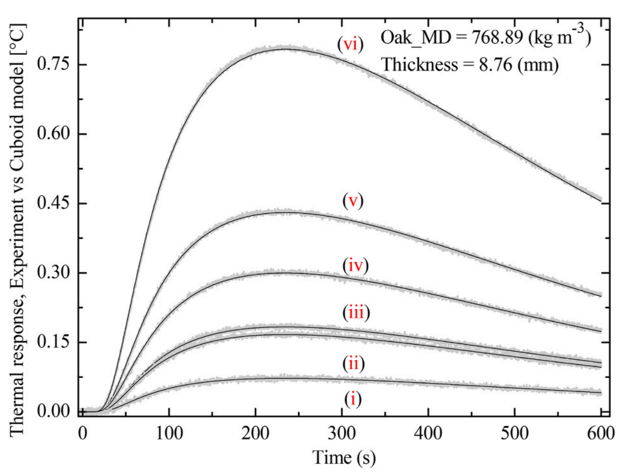

Fig. 6. The comparison of experimentally measured (gray ink) and theoretically calculated (dark black) thermal response curve of Oak MDPB with time duration 600 s are given for different powers of the heat pulse (density 768.89 kg m^{-3}).

used to estimate the availability of the model for these kinds of measurements. For this part of the theoretical calculations, our experimenal results were used as input parameters corresponding exactly to the properties of our samples and measurement regime.

2.1. Pulse transient method (PTM)

The principle of the pulse transition method is based on the generation of a heat pulse by a plane heat source and the recording of the thermal response to the heat pulse. The response to the heat pulse is recorded by a thermocouple, which is located at a distance *h* from the heat source (Fig. 4). The distance *h* represents the active thickness of the cuboid-shaped specimen.

The thermal response shown on the right side of Fig. 4, can be described by the Equation 1 derived from the partial differential equation of the heat conduction, solved for the ideal boundary and initial conditions corresponding to the ideal experimental setup (Kubičár 1990).

$$T(h,t) = \frac{Q}{\lambda\sqrt{\pi\kappa t}}\exp\left(\frac{h^2}{4\kappa t}\right); \quad (1)$$

If the experimental thermal response curve can be described by an ideal model (Eq. (1)), then the thermophysical parameters for the PTM can be calculated using simple formulas derived for the maximum of the thermal response (Kubičár, 1990). These equations represent a one-point evaluation procedure (T_m, t_m).

$$\kappa = \frac{h^2}{2t_m};\ c_p = \frac{Q}{\sqrt{2\pi e}h\rho T_m};\ \lambda = \frac{Qh}{2\sqrt{2\pi e}h\rho T_m};\ Q = RI^2t_0 \quad (2)$$

where *R* is the electrical resistance of the plane heat source, *I* is current, t_0 is the duration of the heat pulse, *Q* is generated heat and the next variables are described above.

An ideal model was derived for a Dirac pulse, but technically in a real experiment, we must use a pulse of a certain duration t_0. In this case, the thermal response function can be corrected to the heat pulse duration (Kubičár, 1990).

$$T(h,t) = \frac{2Q}{c\rho\sqrt{\kappa}}\left[\sqrt{t}\,.i\Phi^*\left(\frac{h}{\sqrt{2\kappa t}}\right) - \sqrt{t-t_0}.\,i\Phi^*\left(\frac{h}{2\sqrt{\kappa(t-t_0)}}\right)\right] \quad (3)$$

where $i\Phi^* = \frac{e^{-ix^2}}{\sqrt{\pi}} - x.erfc(x)$

To evaluate the measurement parameters with the real duration of the pulse t_0, the modified equations for one point evaluation of the thermophysical were derived. The modified relation derived for the maximum of the thermal response have the forms:

$$\kappa = \frac{h^2}{2t_m}(f_a);\ c_p = \frac{Q}{\sqrt{2\pi e}h\rho T_m}(f_c) \quad (4)$$

Where f_a and f_c are the correction factors.

$$f_a = \left(\frac{t_m}{t_0} - 1\right)\ln\left(\frac{\frac{t_m}{t_0}}{\frac{t_m}{t_0} - 1}\right)$$

$$f_c = 2\exp\left(\frac{1}{2}\right)\sqrt{\pi f_a}\cdot\frac{t_m}{t_0}\left\{1/\sqrt{\pi}\left[\exp\left(-\frac{f_a}{2}\right) - \sqrt{\frac{\left(\frac{t_m}{t_0}-1\right)}{t_m}}\exp\left(\frac{t_m}{t_0}\frac{f_a}{2}\left(\frac{t_m}{t_0}-1\right)\right)\right] - \sqrt{\frac{f_a}{2}}\left[\Phi^*\left(\sqrt{\frac{f_a}{2}}\right) - \mathrm{ercf}\left(\frac{t_m}{t_0}\frac{f_a}{2}\left(\frac{t_m}{t_0}-1\right)\right)\right]\right\}$$

The series of Equations (2) and (4) represent a one-point evaluation procedure (Kubičár et al., 2001) (Boháč and Kubičár, 2001) (Boháč et al., 2011).

2.2. Cuboid model (CM)

For the cuboid model, the asymmetric arrangement of the sample geometry takes the form of finite length of cuboids with the same square base but different thicknesses. The model and experimental setup are drawn in Fig. 4. The cuboid model also takes into account the heat transfer coefficient from the free surface of the sample to the surroundings in the lateral direction and the constant temperature and infinite thermal capacity of the heat exchangers located at both ends of the sample.

The sample set consisting of three finite blocks of different lengths was arranged asymmetrically (L1≠L2) on the left and right sides of the heat source (Fig. 4). A plane heat source with zero heat capacity was placed between the first and second parts, and the heat transfer between the heat source and the sample is ideal (α→ ∞). T_0 was the stabilized temperature before the heating pulse was switched on. The thermal response equation (Eq. (5)) derived from the partial differential equation solved for real experimental initial and boundary conditions for the step-wise (sw) heating regime was published in the article (Boháč et al., 2011).

$$T_{sw}(x,y,z,t) = T_0\frac{W}{2}\sum_{n=1}^{\infty}\sum_{m=1}^{\infty}\frac{b_n b_m}{v_{nm}}F(u, v_{nm})\varphi_n\left(\frac{x}{a}\right)\varphi_m\left(\frac{y}{a}\right) \tag{5}$$

where $\varphi_n(s) = \sqrt{\frac{2\beta}{\beta+\sin^2\mu_n}}\cos(\mu_n s), T_0 = \frac{qa}{\lambda}, \beta = \frac{a\alpha}{\lambda}$

$$F_n(u,v) = e^{-2uv}\Phi^*(u-v) - e^{-2uv}\Phi^*(u+v), u = \frac{z}{2\sqrt{kt}}$$

$$w = \frac{\sqrt{kt}}{a}, v_{nm} = w\sqrt{u_n^2 + u_m^2}, b_n = \varphi_n(0)\frac{\sin(\mu_n)}{\mu_n}$$

For the pulse regime the thermal response to the heat pulse is calculated by subtraction of two subsequent step-wise functions shifted on duration of the heat pulse t_0.

$$T_{pulse}(x,y,z,t) = T_{sw}(x,y,z,t) - T_{sw}(x,y,z,t-t_0) \tag{6}$$

A detailed definition of variables was given in the previous article (Boháč et al., 2011). The working accuracy and validity of this model have been successfully demonstrated in many research articles (Boháč et al., 2011, 2023; Tiwari et al., 2021). The model is suitable for small samples when accounting for heat losses from the surface of the sample to the surroundings in the form of heat transfer coefficient α (Boháč et al., 2011).

2.3. Uncertainty and sensitivity coefficients

When evaluating thermophysical data using CM, it is crucial to consider uncertainty and sensitivity coefficients in parameter estimation. Measured data are theoretically and experimentally very susceptible to measurement errors, noise, and other influencing factors. The theory of measurementuncertainty can be fount in ISO/IEC Guide 98-3 (ISO/IEC Guide 98-3). To obtain reliable parameter estimates, it is therefore necessary to consider the uncertainty of the input data, which affects the accuracy of estimating the output parameters of the model. For parameter estimation, we used the Levenberg-Marquardt minimization method, the goal of which is to fit the given model to the experimental thermal response and to minimize the differences between the experiment and the cuboid model. Uncertainty analysis and sensitivity coefficients theory help to determine the optimal time window for estimating the required parameters by introducing a theoretical framework of sensitivity coefficients, applied to any kind of model (Beck and Arnold, 1997).

The residual plot analysis represented by subtraction of the recorded thermal response and the response generated by the model was then used to assess the quality of the fit and the validity of the model Figs. 4–6. The sensitivity coefficients served as a basis for optimizing a suitable time window or time interval for fitting the thermal response. We were interested in a time interval in which the linear correlation of the sensitivity coefficients is zero or negligible. Then we could estimate the given parameters unambogously. If there is a linear correlation between the sensitivity coefficients of thermal conductivity and thermal diffusivity, these parameters cannot be unambiguously evaluated, and the accuracy of determining the estimated parameters is insufficient. As a result, the sensitivity coefficients and their possible correlations in time window intervals provide valuable information for the choice of measurement time and time window for fitting procedures applied to the thermal response.

The sensitivity coefficients are the first derivatives of the thermal response function according to the given parameter a_k within the investigated model $\beta_{a_k} = a_k\frac{\partial T_i(t,x)}{\partial a_k}$ where k means κ, λ, c_p, or α. (ISO/IEC Guide 98-3) (Beck and Arnold, 1997) (Boháč et al., 2000). If the relationship $\gamma(t)$ between a pair of sensitivity coefficients is given by the ratio $\gamma(t) = \beta_\kappa/\beta_c$, on the given time window is a straight line, then the sensitivity coefficients β_κ, β_c on this time window interval are linearly dependent. Therefore, we need to select a time window interval where this relationship is not linear (Boháč et al., 2000). A more advanced analysis of sensitivity coefficients for cuboid model was published in our previous paper (Boháč et al., 2011), where a corresponding theory was introduced to calculate the uncertainty for the cuboid model. An equation of the form $u_r(a_k)^2 = C_{kT}^2\frac{u(T)^2}{a_k^2} + \sum_{j=1}^{N_b}\nu_{kj}^2 u_r(b_j)^2$, was derived for the uncertainty (u_r represents uncertainty matrix). Mathematical steps of the derivation of this equation, used nomenclature and the corresponding basic theory have been published in papers (Boháč et al., 2011), (ISO/IEC Guide 98-3; Beck and Arnold, 1997).

3. Results and discussions

The standard experiment for Turkey oak MDPB and HDPB was performed in a dry state under room conditions. The total time of the transient record of the thermal response was 600 s. The experimental data were evaluated by the cuboid model for PTM. Simple one point procedure relations derived for the maximum of the thermal response were used to calculate the values of κ, λ, and c (Eq. (4)), which serves as input guess parameters for fitting by the cuboid model.

The estimation of thermophysical parameters from the experimental thermal response curves was successful. The thermal response curves measured at different thermal pulses are plotted in Fig. 5, and Fig. 6 to illustrate the quality of the fitting.

For higher data reliability at least 5 measurements for each set of pulse width and current were performed. Subsequently, for better statistics of data, approximately 30 measurements were performed in total.

It is clear from Table 1, Fig. 5, and Fig. 6 that the maximum of thermal responses for T_m for MDPB at all pulse powers reach higher values than for HDPB. The times to reach the maximum t_m for pulse powers (ii/1 A, 2.5 s) and (iii/1.5 A, 1 s) are longer for MDPB than HDPB, and for all other powers, the time to reach the maximum was shorter for MDPB than for HDPB. However, the differences are not large and the interval of t_m values for the used power range of heat pulses 2873 ÷ 30942 J m^{-2} for HDPB and 2915 ÷ 31450 J m^{-2} for MDPB was statistically almost the same, namely 232 ÷ 238.4 s for MDPB and 233 ÷ 237.8 s for HDPB. These time intervals are almost identical and can be attributed to the statistical dispersion of the measurements.

Shorter times to reach the maximum are related to higher values of thermal conductivity and lower thickness of the material. The magnitude of the specific heat capacity values for a given material density is proportional to the height of the thermal response T_m. Denser HDPB samples should have specific heat capacity values lower, but they are, despite expectations higher, which may be a result of the complexity of the structure of the given composite. The value of the thermal response height T_m for HDPB is smaller than that for MDPB. It is evident that MDPB retains heat better and with the same amount of supplied heat we can heat them to a higher temperature. Lighter MDPB samples have a lower density and probably contain more pores.

The reason for the shift of the thermal response maximum of HDPB and MDPB samples with time is also influenced by the different thicknesses of the MDPB/HDPB samples (8.76 mm/9.16 mm). If we had an MDPB sample 0.4 mm thicker (the same as HDPB), the time interval of the maximum thermal response would be shifted to higher times, which again corresponds to the phenomenon of longer heat accumulation by the MDPB material. Other factors that influence the shape of the thermal response are mainly sample dimensions, inhomogeneous structure, interfaces, and imperfect thermal contact between parts of the sample set, which is usually caused by the poor flatness of the sample surfaces. Also, when a shorter duration of the heat pulse with lower heat energy is expected, the thermal readings would be lower.

After performing the measurements, we obtained thermophysical parameters calculated by using one point evaluation procedure. These data are affected by heat losses, so they only serve as initial guesses for fitting procedures to estimate parameters using the cuboid model. Fig. 7 shows a graph of calculated statistical averages of thermophysical parameters for different energies of heat pulses.

The reason for measuring the thermophysical properties of these materials at different pulse powers was to investigate possible disturbance effects that are usually dependent on the temperature. For example, the influence of the uneven surface of the sample parts causes an additional thermal resistance to heat transfer, represented by the thermally dependent coefficient of heat transfer from the heat source to the sample. If such a disturbing effect is present during the measurement, then the evaluated data for different pulse powers are not constant and tends to increase the dispersion of the measured data. Thermophysical parameters cannot then be determined unambiguously. If the measured data corresponds to the statistical measurement error, then we can declare that the data are reliable, which is also our case Fig. 7. Moreover, the physical properties of the materials and systems are categorized as intensive or extensive. An example of an intensive state variable is the specific heat capacity, which is an intensive property of the matter and does not depend on the geometry and amount of the material and should not depend on the amount of the heat used for its diagnosis either. If we would obtain very different values for different pulse powers, then this quantity should be extensive, which is not in accordance with the basic principles of physics.

We compared the measurement result of MDPB with HDPB for different pulse powers. The statistically processed resulting data are graphically represented as a function of the heat pulse energy in Fig. 7, Table 2, and in Table 3 are given numerically. Thermophysical parameters plotted on Fig. 7 for HDPB are on the right and for MDPB on the left.

The error bar for each series of measurements for different pulse energies represents the standard deviation error calculated from a series of measurements for the same pulse parameters. For a given range of heat pulse powers, the data are relatively stable, mainly for HDPB. The error bar decreases with increasing heat output in both cases. Larger measurement errors and data scattering for MDPB are associated with the flatness of the sample surface. While the HDPB was perfectly planar, the MDPB has small gaps at the corners of the sample that increase thermal resistance of the heat source-sample interface. The size of the percentual errors is small and for all basic thermophysical parameters are lower than 0.71% for HDPB and lower than 1.32% for MDPB. Only in the case of the heat transfer coefficient the percentual error is in the range 6–47% for HDPB and in the range 15–319% for MDPB. For example, the mean value and standard deviation of the heat transfer coefficient at a pulse energy 3.14*10^4 J m^{-2} (2.5s and 2A) for HDPB is 5.42 ± 0.31 (±5.7%) and for MDPB 11.21 ± 1.71 (±15.3%). The increased uncertainty for the heat transfer coefficient is associated with its low sensitivity coefficient values.

In general, the scatter of the data decreases with increasing heat pulse energy for all data. This can be explained by analyzing the sensitivity coefficients, the value of which increases with increasing pulse energy and thus with the height of the thermal response. Therefore, the

Table 1
Maximum point parameters (T_m, t_m) of the thermal response curve measured for a series of currents of 1, 1.5 and 2A and a heat pulse duration of 1 and 2.5s for oak HDPB and MDPB (thickness h = 9.15 mm and 8.76 mm respectively).

Maximum point parameters	Current and Heat pulse duration					
	(i) 1A, 1s	(ii) 1 A, 2.5s	(iii) 1.5 A, 1s	(iv) 1.5 A, 2.5s	(v) 2 A, 1s	(vi) 2 A, 2.5s
$T_{m\ \mathrm{MDPB}}$ (°C)	0.07	0.18	0.16	0.43	0.30	0.78
$t_{m\ \mathrm{MDPB}}$ (s)	232.0	234.8	238.4	233	232.8	233.4
$T_{m\ \mathrm{HDPB}}$ (°C)	0.06	0.15	0.14	0.36	0.25	0.66
$t_{m\ \mathrm{HDPB}}$ (s)	235.6	233.8	233	237.4	234.6	237.8
$\Delta T_{m\ \mathrm{MD\text{-}HD}}$ (°C)	0.01	0.03	0.02	0.07	0.05	0.12
$\Delta t_{m\ \mathrm{MD\text{-}HPD}}$ (s)	−3.6	1.0	5.4	−4.4	−1.8	−4.4

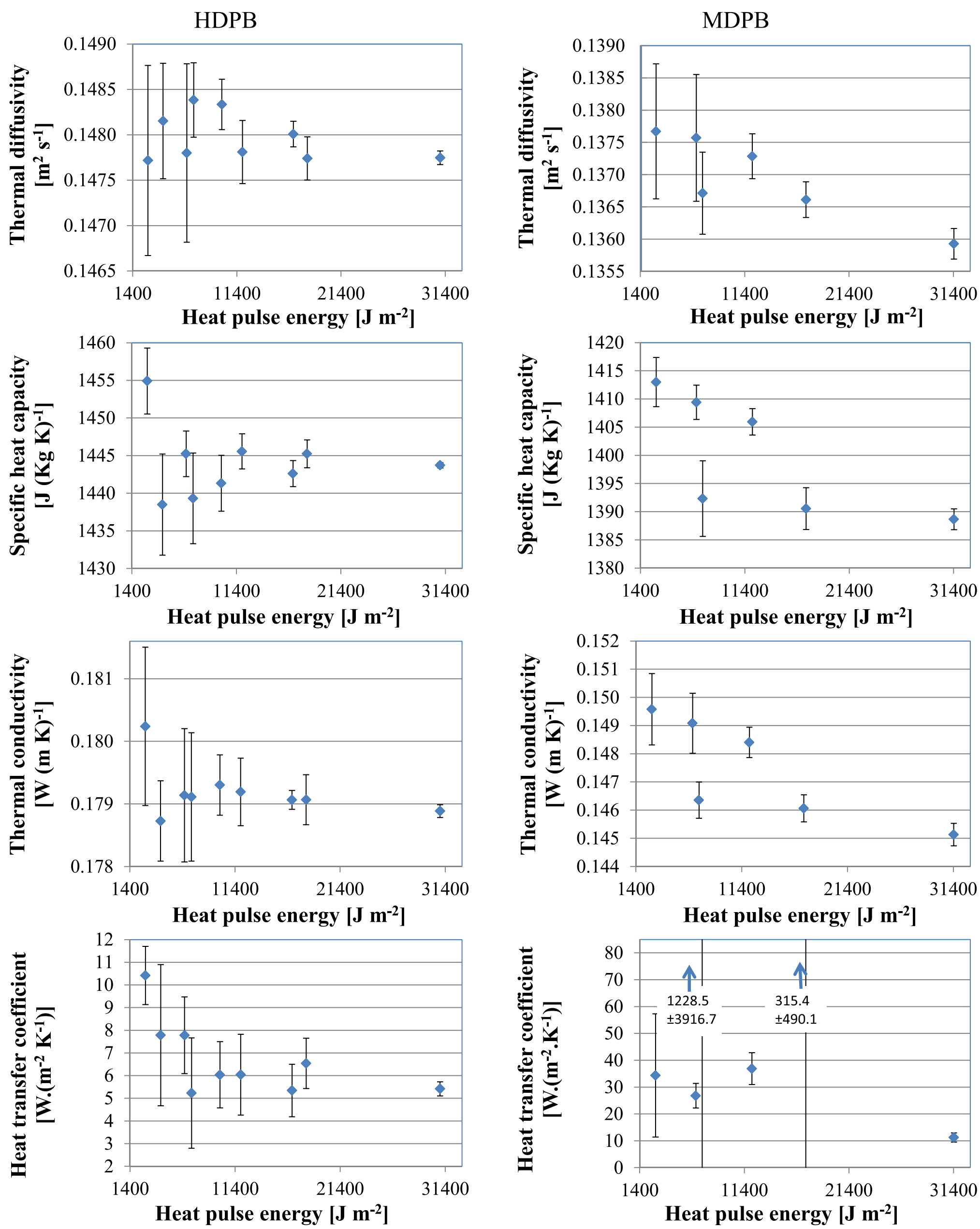

Fig. 7. The plot of dependency of thermophysical parameters on heat pulse power for oak HDPB (left) and MDPB (right). For a given range of heat pulse powers, the data are relatively stable, mainly for HDPB. The error bar decreases with increasing heat output in both cases. Generally, the measurement uncertainty is bigger for MDPB. The last graph with heat transfer coefficient of MDPB (right) was plot in fine scale to.be comparable with HDPB on the left.

Table 2
The calculated statistical average of κ, C, λ, α, and Q, with a standard deviation given for of Oak MDPB obtained using CM.

Pulse Width (s)	Current (A)	κ × 10 $^{-7}$ [m^2 s^{-1}]	StDev κ × [m^2 s^{-1}]	c [J (kg K) $^{-1}$]	StDev c [J (kg K) $^{-1}$]	λ [W (m K) $^{-1}$]	StDev λ [W (m K) $^{-1}$]
	1.0	0.1377	0.00079	1413.00	10.665	0.1496	0.00197
1.0 s	1.5	0.1376	0.00031	1409.47	4.676	0.1491	0.00081
	2.0	0.1373	0.00022	1405.94	1.386	0.1484	0.00037
	1.0	0.1367	0.00033	1392.32	2.568	0.1464	0.00042
2.5 s	1.5	0.1366	0.00028	1390.55	3.566	0.1461	0.00037
	2.0	0.1359	0.00012	1388.65	1.093	0.1451	0.00025

Pulse Width (s)	Current (A)	α [W (m^{-2} K^{-1})]	StDev α [W (m^{-2} K^{-1})]	Q [J m^{-2}]	StDev Q [J m^{-2}]
	1.0	34.34	22.966	2915.0	0.23
1.0 s	1.5	26.79	4.589	6768.1	0.85
	2.0	36.87	5.923	12129.2	2.08
	1.0	1228.54	3916.756	7368.1	1.52
2.5 s	1.5	315.41	490.068	17274.5	2.25
	2.0	11.21	1.712	31437.5	12.14

Table 3
The calculated statistical average of κ, C, λ, α, and Q, with a standard deviation given for Oak HDPB obtained using CM. (Boháč et al., 2023).

Pulse Width (s)	Current (A)	$\kappa \times 10^{-7}$[m^2 s^{-1}]	StDev $\kappa \times 10^{-7}$ [m^2 s^{-1}]	c [J (kg K)$^{-1}$]	StDev c [J (kg K)$^{-1}$]	λ [W (m K) $^{-1}$]	StDev λ [W (m K) $^{-1}$]
1.0 s	1.0	0.1477	0.00105	1454.9	4.375	0.18024	0.00126
	1.5	0.1478	0.00098	1445.2	3.036	0.17914	0.00106
	2.0	0.1478	0.00035	1445.6	2.336	0.17919	0.00054
2.5 s	1.0	0.1482	0.00064	1438.5	6.716	0.17873	0.00064
	1.5	0.1483	0.00028	1441.3	3.718	0.17930	0.00048
	2.0	0.1477	0.00024	1445.2	1.849	0.17907	0.00040

Pulse Width	Current (A)	α [W (m^{-2} K^{-1})]	StDev α [W (m^{-2} K^{-1})]	Q [J m^{-2}]	StDev Q [J m^{-2}]
1.0 s	1.0	10.42	1.285	2874.5	1.493
	1.5	7.78	1.695	6596.2	8.551
	2.0	6.04	1.786	11942.8	10.696
2.5 s	1.0	7.79	3.113	4327.4	2.158
	1.5	6.04	1.460	9965.8	5.038
	2.0	6.54	1.113	18167.7	21.781

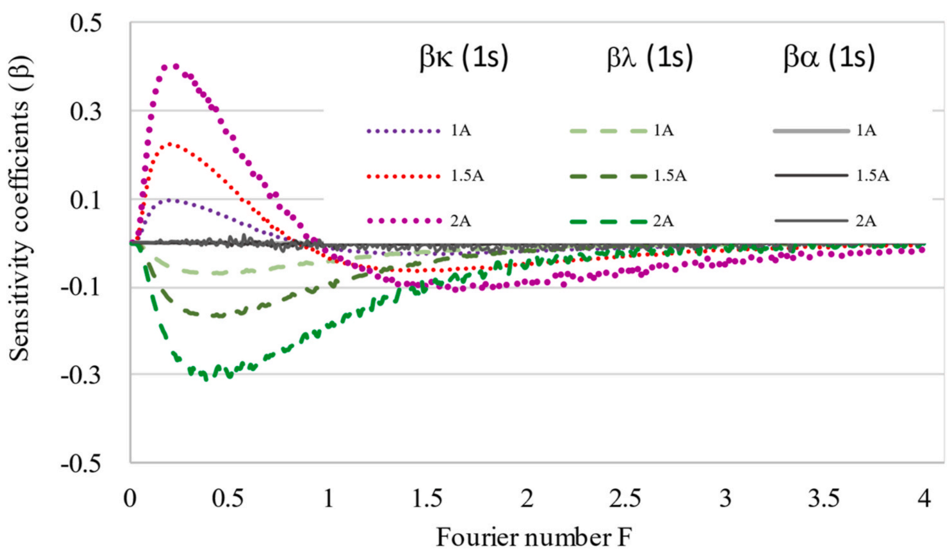

Fig. 8. The sensitivity coefficient βκ, βλ, and βα plotted against dimensionless time expressed as a Fourier number. Theoretical calculations of sensitivity coefficients are given for pulses generated by current 1A, 1.5A and 2A. The values of the sensitivity coefficients increase with the increase in the pulse power.

values obtained for higher energy values are estimated more unambiguously. Nevertheless, due to the very low percentage error in the data, we consider the values to be reliable and correspond to the usual measurement error.

The thermophysical data obtained from two different densities have shown negligible dependence on selected input heat power for thermal diffusivity and thermal conductivity. Additionally, higher-density particleboard has slightly higher thermophysical parameters than medium density particleboards. This suggests a robustness in the measured values, regardless of the heat pulse power used for the experiment. From the general theory of basic data consistency condition $\lambda = \kappa\rho c$ the higher the density the higher the thermal transport properties, e.g thermal diffusivity and thermal conductivity. On the contrary, with increasing density, the order of atomic, molecular or particle arrangement is higher and thus the free energy of the system is lower and the specific heat capacity values should decrease. It follows from one of the consequences of the second law of thermodynamics that the specific heat capacity is a measure of the arrangement of the system.

It was observed also that the estimation of the heat transfer coefficient parameter with standard deviation has the highest uncertainty, as indicated by the sensitivity coefficient analysis described in the literature (ISO/IEC Guide 98-3) (Beck and Arnold, 1997).

The optimization of the parameters of the pulse power, i.e., the power of the pulse and its duration used for the experiment, was analyzed using the theory of sensitivity coefficients and the analysis of uncertainties in parameter estimation. Fig. 8 represent the plot of sensitivity coefficients for β_κ, β_λ, and β_α against dimensionless time expressed as a Fourier number ($F = (k{*}t)/h^2$). Theoretical calculation of sensitivity coefficients were performed for pulses generated by current 1A, 1.5A and 2A. The values of the sensitivity coefficients increase with the increase in the pulse power. Figs. 8 and 9 shows the time courses of the sensitivity coefficients for all used current combinations for pulse

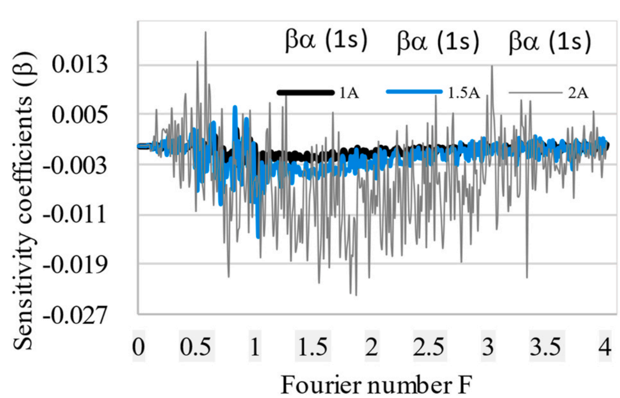

Fig. 9. Sensitivity coefficient of heat transfer coefficient βα calculated for the current of 1A and different pulse durations. The magnitude of the negative peak increases to −0.002 for 1A, −0.017 for 1.5A and −0.024 for 2A.

durations of 1 s. The graph clearly shows an increase in sensitivity with an increase in current height and increasing time. The thermal diffusivity and thermal conductivity sensitivity coefficients reach their maximum at 0.25 F and 0.5 F. The sensitivity coefficient for the coefficient of heat transfer to the surrounding has a maximum of around 1.5 F. Its course increases with increasing time in accordance with the assumption that the effect of heat transfer to the surrounding from the free surface of the sample in the lateral direction increases with time. The higher the applied current and the longer the scanning time of the thermal response, the higher were the maximum values of the sensitivity coefficients depending on the increasing dimensionless time - Fourier number. After reaching the maximum, their values drop to zero due to long thermal response times. The conclusion of this analysis is that there is no reason to continue scanning the thermal response beyond this time.

The analysis of time-dependent transport phenomena using the Fourier number allows us to compare different measurement conditions in the analysis of wood composite samples. Conversion of real time to Fourier number unifies the characteristic time points of the sensitivity coefficient maximum. For all materials, the maximum should be found at the same value of F. This makes it possible to compare different materials and find the best sensitivity of the model to different experimental conditions. This method helps to find the best optimal parameters for the experiment. Fourier number is defined as the ratio of time t, to the characteristic time scale for heat diffusion t_d. For heat transported through a sample material of thickness h with known thermal diffusivity κ, the diffusion time scale is $t_d = h^2/\kappa$, so that $F = \kappa.t/h^2$. In Fig. 9, the sensitivity coefficient for the heat transfer coefficient βα is shown separately to provide a more detailed resolution of the effect of increasing sensitivity coefficient values with increasing pulse power.

During recording of the thermal response to the heat pulse, the generated heat takes a longer time to penetrate the sample and reach the thermocouple. During this process, however, the effect of heat loss from the surface of the sample in the lateral direction will begin to manifest itself. The heat flow that heats the sample at the location of the thermocouple located at the interface of sample parts II and III is divided into axial and lateral, which ultimately reduces the height of the thermal response. Without including this effect in the model, it would not be possible to fit the thermal response curve as plotted in Figs. 5, and Fig. 6.

When the sensitivity coefficients increase with time with a positive or negative maximum and then begin to decrease, the positions of their maxima indicate the optimal range of the time window for parameter estimation by the given model. This means that the optimum time should be 1.5 F, e.g. the maximum βα. The uncertainty of parameters estimation is connected with this analysis. Consequently, the calculated relative uncertainty of the estimated parameters κ, λ and α decreases with time. The consideration of heat losses from the surface in the form of the heat transfer coefficient α is crucial because it affects the height of the measured thermal response illustrated in Figs. 5, and Fig. 6. Higher values of the coefficients of sensitivity of thermal diffusivity and thermal conductivity are related to lower uncertainty of the estimation of these parameters, and their values are determined unambiguously with a high reliability. The relatively large variance of the values of the heat transfer coefficient for lower pulse powers is related to its small sensitivity coefficients and, consequently, the high value of the relative uncertainty of determining this parameter, so this parameter is not possible to estimate so unambiguously. However, the uncertainty of the estimate for this parameter decreases with increasing heat pulse power, e.g., higher currents and longer duration of the heat pulse.

In the future, it may be necessary to evaluate the context and other relevant factors and interpret the implications in the case of a low sensitivity of parameter. Fig. 10 shows the calculated relative uncertainties of the free parameters of the cuboid model for thermal diffusivity, thermal conductivity, and heat transfer coefficient from the sample surface in the lateral direction as a function of dimensionless time F for all heat puwers used in experiment. The relative uncertainty of determining these parameters decreases with the increasing time of the thermal response scan. At values above 0.5 F, the decrease is no longer so significant. Therefore, the measurement until 200s–300s is required for the measurement to rich sufficient accuracy. From the theoretical point of view the coefficient of sensitivity βα has an extremum in negative values approximately at 1.5F (819 s). As a compromise, we used 1.1 F (600 s) for total time recording to obtain accurate measurements and account for heat loss from the sample surface. Above this value, the uncertainty decreases very slowly, so there is practically no reason to extend the measurement time.

It is clear from Fig. 9 that the sensitivity coefficients βα in response to a heat pulse are not sensitive to changes for small pulse powers. The time courses of the uncertainties of parameter estimation help to determine the setting of experimental conditions to achieve the required accuracy of measurements. In the future, context and other relevant factors may need to be evaluated and the consequences of low sensitivity interpreted.

The sensitivity coefficients initially increase with, reaching a maximum before gradually decreasing. Simultaneously, the relative uncertainty in the estimation of coefficients κ, λ and α decreases with time. Incorporating heat losses from the surface in the form of the heat transfer coefficient α is crucial because it affects measured thermal response illustrated in Figs. 5, and Fig. 6. Higher sensitivity coefficients for thermal diffusivity and thermal conductivity correspond to more precise parameter estimation, providing reliable results. Conversely, the heat transfer coefficient exhibits a relatively large variance in values due to smaller sensitivity coefficients, resulting in higher relative uncertainty when estimating this parameter. However, this uncertainty decreases with increased pulse power, such as higher currents and longer heat pulse durations. For our theoretical analysis and assumptions, we also tried to check the implications of increasing input current and heat pulse energy using the same thermophysical parameters in the concern of reducing uncertainty errors and corresponding sensitivity analysis.

We theoretically analyzed how the results would change when using higher values of heat pulse energy by increasing the pulse current to 3A or 5A. The calculations were carried out using thermophysical parameters that we obtained experimentally and are presented in Table 3. The

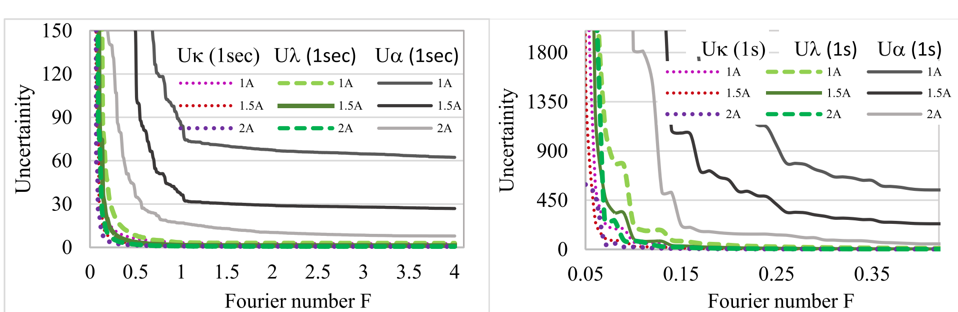

Fig. 10. The plot of the analysis of calculated uncertainties for thermal diffusivity and thermal conductivity and heat transfer coefficient as a function of dimensionless time up to 4F - Fourier number ($F = (k^*t)/h^2$). Parameters for the calculations were: Pulse width $t_0 = 1$ s, current values 1A, 1.5A, 2A and thickness 8.71 mm.

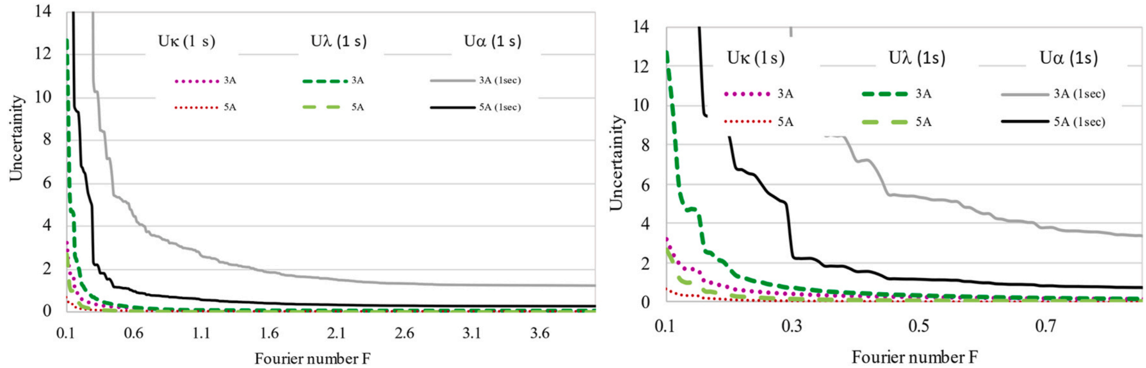

Fig. 11. The analysis of relative uncertainty for hypothetical values of currents and energy of heat pulses within the dimensionless time scale F consistent with previous results. To calculate the energy of the heat pulse 27030 (J m^{-2}) and 75080 (J m^{-2}) as input parameters, the duration of the heat pulse 1s and the currents 3A and 5A, as well as the area of the heat source (0.0025 m^2), were used. On the right, a clear image of all thermophysical parameters was drawn, registering the point of change in the bend of the curve in relation to the time when the uncertainty value starts to decrease much more slowly. In general, this shows that the higher the input current, the greater the decrease in uncertainty observed with increasing Fourier time.

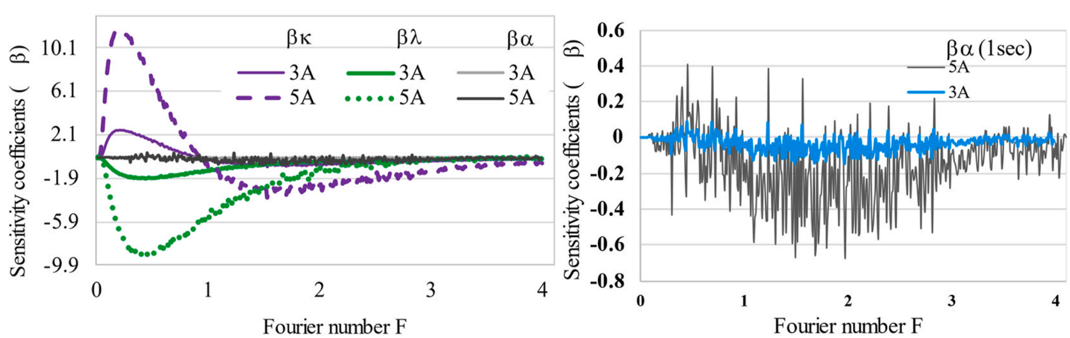

Fig. 12. The analysis of sensitivity coefficients for hypothetical values of currents and energy of heat pulses within the dimensionless time scale F consistent with previous results. The same input parameters as in Fig. 11 were used to calculate the thermal pulse energy of 27030 (J m^{-2}) and 75080 (J m^{-2}).

results can be seen in Figs. 11 and 12, which, according to the theory, meet our assumption of an increase in the values of the sensitivity coefficients and a decrease in the uncertainty values. Experimentally, however, the pulse performance is limited by the hardware options of the RT-Lab measuring unit and probably also by the problem of the flammability of the HDPB and MDPB samples and their thermal stability, because of their carbonization or overheating could occur. The sensitivity coefficients of all parameters for increased pulse power in Fig. 11 has increased up to two or three times compared to Fig. 9.

The heat transfer coefficient is a crucial parameter for the cuboid model, as it largely characterizes the relative uncertainty of determination of other parameters as well. This parameter, as discussed in the model theory chapter, helps to account for the heat loss effect from the sample surface to the surroundings. It is a critical issue in longer thermal response measurements. The mentioned analysis of the uncertainties calculated using the sensitivity coefficients of the free parameters of the model helps to compare their possible linear dependence and to determine the time interval on the thermal response curve where the parameters can be unambiguously estimated and where the uncertainty is minimal, or at least sufficient. As a result, accurate parameter estimation becomes challenging.

4. Conclusions

The investigation of the thermophysical properties of MDPB was successfully carried out, covering the original purpose of the research. The thermophysical parameters of the MDPB were studied by means of the pulse transient method using the cuboid model. Measurements were performed under room conditions. These data were compared with the data obtained at HDPB published in (Boháč et al., 2023). Parameters such as thermal diffusivity, thermal conductivity, and specific heat capacity were calculated with statistical differences of less than 1.32% and less than 40% for the real values of the heat transfer coefficient.

In total, more than 100 measurements of oak HDPB and MDPB were statistically processed to calculate average values of thermophysical parameters. The comparison of the data proved beneficial in providing an overview of strategic opportunities for the variation with the power of the generated heat pulses. Comparing the results of measurements and calculated statistical errors with the analyzed uncertainties of the parameters estimated by the cuboid model made it possible to better analyze the effect of the change in experimental conditions on the resulting uncertainty of parameter determination. The Marquardt-Levenberg minimization procedure was used to estimate the parameters using the cuboid model. In addition, using the theory of sensitivity coefficients and uncertainty calculations, the availability of the cuboid model for the pulse transient method was successfully confirmed.

An investigation of the thermophysical parameters of two types of turkey oak chipboards revealed the significant role of the thermal pulse energy used in the measurements to check possible effect of thermal resistance, as well as the optimization of the thermal response time window used to estimate the parameters by fitting using a cuboid model. This knowledge will contribute to the development of knowledge in the field of thermal behavior of wood and its products for application in house construction. The results of this research will be used in the construction of sustainable building envelopes.

Declaration of competing interest

The authors declare that they have no known competing financial interests or personal relationships that could have appeared to influence the work reported in this paper.

Data availability

Data will be made available on request.

Acknowledgments

This research was supported by the Scientific Grant Agency – VEGA of the Ministry of Education, Science, Research and Sports of the Slovak Republic under project No. 1/0714/21, Research of selected properties of sustainable insulation materials with potential for use in wooden buildings. This work was also supported by the Slovak Research and Development Agency under contract APVV-19-0269 and SK-CZ-RD-21-0100. This study was carried out within the Agritech National Research Center and received funding from the European Union Next-GenerationEU (PIANO NAZIONALE DI RIPRESA E RESILIENZA (PNRR) – MISSIONE 4 COMPONENTE 2, INVESTIMENTO 1.4 – D.D. 1032 June 17, 2022, CN00000022).

References

Akinyemi, B.A., Olamide, O., Oluwasogo, D., 2019. Formaldehyde free particleboards from wood chip wastes using glutaraldehyde modified cassava starch as binder. Case Stud. Constr. Mater. 11, e00236 https://doi.org/10.1016/j.cscm.2019.e00236.

Asdrubali, F., Ferracuti, B., Lombardi, L., Guattari, C., Evangelisti, L., Grazieschi, G., 2017. A review of structural, thermo-physical, acoustical, and environmental properties of wooden materials for building applications. Build. Environ. 114, 307–332. https://doi.org/10.1016/j.buildenv.2016.11.004.

Beck, J.V., Arnold, K.J., 1997. Parameter Estimation in Engineering and Science". John Wiley & Sons, Inc., New York, London, Sydney, Toronto https://doi.org/10.1002/aic.690240233.

Boháč, V., Kubičár, Ľ., 2001. Investigation of surface effects on PMMA by pulse transient method. In: Thermophysics 2001. Proceedings of the Meeting of the Thermophysical Society, p. 21. Retrieved from. http://www.tpl.fpv.ukf.sk/engl_vers/thermophys/thermophys_01.pdf.

Boháč, V., Gustavsson, M.K., Kubičár, L., Gustafsson, S.E., 2000. Parameter estimations for measurements of thermal transport properties with the hot disk thermal constants analyzer. Rev. Sci. Instrum. 71 (6), 2452–2455. https://doi.org/10.1063/1.1150635.

Boháč, V., Dieška, P., Vretenár, V., Greif, V., 2011. Model for cuboid shape samples and its analysis used for measurements of thermophysical properties of sandstone. Meas. Sci. Rev. 11 (6), 192–197. https://www.measurement.sk/2007/S3/Bohac2.pdf.

Boháč, V., Tiwari, R., Krišťák, L., Todaro, L., Lo Giudice, V., Vretenár, V., 2023. Thermal properties of oak high density particle board measured by the pulse transient method for different heat pulse energy. http://thermophysics.fch.vut.cz/2022/pdf/Abstracts_Thermophysics%202022.pdf.

Božiková, M., Kotoulek, P., Bilčík, M., Kubík, Ľ., Hlaváčová, Z., Hlaváč, P., 2021. Thermal properties of wood and wood composites made from wood waste. Int. Agrophys. 35 (3), 251–256. https://doi.org/10.31545/intagr/142472.

Çavuş, V., Şahin, S., Esteves, B., Ayata, U., 2019. Determination of thermal conductivity properties in some wood species obtained from Turkey. Bio 14 (3), 6709–6715. https://doi.org/10.15376/biores.14.3.6709-6715.

Darwish, E.A., Eldeeb, A.S., 2023. Utilizing agro-industrial wastes panels in developing cost-efficient thermally insulating wall claddings for residential energy retrofitting in Egypt. Energy Built Environ. https://doi.org/10.1016/j.enbuild.2023.07.055.

Essid, S., Hegde, V.J., Mahieu, A., Bizet, L., Leblanc, N., Saouab, A., 2021. Comparison of the properties of flax shives based particleboards prepared using binders of bio-based lignin and partially bio-based epoxy resin. Int. J. Adhesion Adhes. 109, 102915 https://doi.org/10.1016/j.ijadhadh.2021.102915.

EUROTECH Vacuum Technologies. https://eurotech-vacuum-technologies.com/vacuum-technology-for-industries/material-of-lifted-workpieces/wooden-board-material-furniture-industry/.

Faouel, J., Mzali, F., Jemni, A., Nasrallah, S.B., 2012. Thermal conductivity and thermal diffusivity measurements of wood in the three anatomic directions using the transient hot-bridge method. J. Spec. Topics Rev. Porous Media: Int. J. 3 (3), 229. https://doi.org/10.1615/specialtopicsrevporousmedia.v3.i3.40.

Ghobadi, M., Sepasgozar, S.M., 2023. Circular economy strategies in modern timber construction as a potential response to climate change. J. Build. Eng., 107229 https://doi.org/10.1016/j.jobe.2023.107229.

Gustafsson, S.E., 1991. Transient plane source techniques for thermal conductivity and thermal diffusivity measurements of solid materials. Rev. Sci. Instrum. 62 (3), 797–804. https://doi.org/10.1063/1.1142206. https://fu.sav.sk/veda-a-vyskum/infrastruktura/termofyzikalne-laboratorium/. https://www.iso.org/standard/60063.html.

Hua, L.S., Chen, L.W., Geng, B.J., Kristak, L., Antov, P., Pędzik, M., et al., 2022. Particleboard from agricultural biomass and recycled wood waste: a review. J. Mater. Res. Technol. https://doi.org/10.1016/j.jmrt.2022.07.055.

ISO/IEC Guide 98-3. Uncertainty of measurement — Part 3: Guide to the expression of uncertainty in measurement (GUM:1995). https://www.iso.org/standard/50461.htm.

Ji, R., Zhang, Z., Liu, L., Wang, X., 2014. Development of the random simulation model for estimating the effective thermal conductivity of insulation materials. Build. Environ. 80, 221–227. https://doi.org/10.1016/j.buildenv.2014.06.006.

Karawacki, E., Suleiman, B.M., ul-Haq, I., Nhi, B., 1992. An extension to the dynamic plane source technique for measuring thermal conductivity, thermal diffusivity, and specific heat of dielectric solids. Rev. Sci. Instrum. 63, 4390. https://doi.org/10.1063/1.1143434.

Kotoulek, P., Malínek, M., Božiková, M., Hlaváč, P., Bilčík, M., Hlaváčová, Z., Csillag, J., 2018, 2018 Biblid 22 (2). Basic thermal properties and geometric characteristics of wood and oriented strand boards used in low-energy buildings 1821-4487, pp. 73–75. UDK: 62-664.

Kristak, L., Antov, P., Bekhta, P., Lubis, M.A.R., Iswanto, A.H., Reh, R., et al., 2023. Recent progress in ultra-low formaldehyde emitting adhesive systems and formaldehyde scavengers in wood-based panels: a review. Wood Mater. Sci. Eng. 18 (2), 763–782. https://doi.org/10.1080/17480272.2022.2024201.

Kubičár, L., 1990. Pulse Method of Measuring Basic Thermophysical Parameters.

Kubičár, Ľ., Boháč, V., Gaal, PS., Apostolescu, DE., Review of several dynamic methods of measuring thermophysical parameters. 1999/1/11 Journal:Proc. Of 24th Int. Conf. on Thermal Conductivity/12th Int. Thermal Expansion Symposium", ed. PS Gaal, DE Apostolescu, Lancaster: Technomic Publishing Company, 135-149..

Kubičár, Ľ., Boháč, V., Vretenár, V., 2001. Contact constriction and free surface effects in pulse transient method. In: Thermophysics 2001, Proceedings of the Meeting of the Thermophysical Society, pp. 27–35. Retrieved from. http://www.tpl.fpv.ukf.sk/engl_vers/thermophys/thermophys_01.pdf.

Lagüela, S., Bison, P., Peron, F., Romagnoni, P., 2015a. Thermal conductivity measurements on wood materials with transient plane source technique. Thermochim. Acta 600, 45–51. https://doi.org/10.1016/j.tca.2015.01.009.

Lagüela, S., Bison, P., Peron, F., Romagnoni, P., 2015b. Thermal conductivity measurements on wood materials with transient plane source technique. Thermochim. Acta 600*, 45–51. https://doi.org/10.1016/j.tca.2014.11.021.

Mvondo, R.R.N., Damfeu, J.C., Meukam, P., Jannot, Y., 2020. Influence of moisture content on the thermophysical properties of tropical wood species. Heat Mass Tran. 56, 1365–1378. https://doi.org/10.1007/s00231-019-02710-z.

Reddy, K.S., Jayachandran, S., 2017. Investigations on design and construction of a square guarded hot plate (SGHP) apparatus for thermal conductivity measurement of insulation materials. Int. J. Therm. Sci. 120, 136–147. https://doi.org/10.1016/j.ijthermalsci.2017.06.014.

Schiavoni, S., Bianchi, F., Asdrubali, F., 2016. Insulation materials for the building sector: a review and comparative analysis. Renew. Sustain. Energy Rev. 62, 988–1011. https://doi.org/10.1016/j.rser.2016.04.034.

Slováčková, B., 2021. Thermal conductivity of spruce, beech and oak heartwood degraded with Trametes versicolor L. Lloyd. Acta Facultatis Xylologiae. https://doi.org/10.17423/afx.2021.63.1.01.

Solt, P., Konnerth, J., Gindl-Altmutter, W., Kantner, W., Moser, J., Mitter, R., van Herwijnen, H.W., 2019. Technological performance of formaldehyde-free adhesive alternatives for particleboard industry. Int. J. Adhesion Adhes. 94, 99–131. https://doi.org/10.1016/j.ijadhadh.2019.05.008.

Štofanik, V., Markovič, M., Boháč, V., Dieška, P., Kubičár, Ľ., 2007. RT-lab - the equipment for measuring thermophysical properties by transient methods. Meas. Sci. Rev. 7, 15–18. Section 3 1. http://www.measurement.sk/2007/S3/Stofanik.pdf.

Taib, M.N.A.M., Antov, P., Savov, V., Fatriasari, W., Madyaratri, E.W., Wirawan, R., et al., 2022. Current progress of biopolymer-based flame retardant. Polym. Degrad. Stabil. 110153 https://doi.org/10.1016/j.polymdegradstab.2022.110153.

Taoukil, D., El bouardi, A., Sick, F., Mimet, A., Ezbakhe, H., Ajzoul, T., El abbassi, I., 2013. Moisture content influence on the thermal conductivity and diffusivity of wood–concrete composite. Construct. Build. Mater. 48, 104–115. https://doi.org/10.1016/j.conbuildmat.2013.06.067.

Tiwari, R., Boháč, V., Dieška, P., Götzl, G., 2021. The non-planar surface of carbonate rock sample affecting the behaviour of thermal response and the measurement of Thermophysical parameters by Pulse Transient Technique. Therm. Sci. Eng. Prog. 24, 100927 https://doi.org/10.1016/j.tsep.2021.100927. ISSN 2451-9049.

Xu, Youjie, Wang, Donghai, 2019. Integrated Processing Technologies for Food and Agricultural By-Products. https://www.sciencedirect.com/topics/agricultural-and-biological-sciences/particleboards.

Yang, I., Kim, D., Lee, S., Jang, H., 2019. Construction and calibration of a large-area heat flow meter apparatus. Energy Build. 203, 109445 https://doi.org/10.1016/j.enbuild.2019.109445.

Yang, Y., Chen, Z., Wu, T.V., Sempey, A., Batsale, J.C., 2022. In situ methodology for thermal performance evaluation of building wall: a review. Int. J. Therm. Sci., 107687 https://doi.org/10.1016/j.ijthermalsci.2022.107687.

Yapici, F., Ozcifci, A., Esen, R., Kurt, S., 2011. The effect of grain angle and species on thermal conductivity of some selected wood species. Bio 6 (3), 2757–2762. https://doi.org/10.15376/biores.6.3.2757-2762.

Zhao, J., Feng, S., Kou, Z., Meissner, F., Ruisinger, U., Grunewald, J., 2023. Characterization of hygrothermal properties of two wood species: the impact of anisotropy on their thermal and moisture behaviors. Construct. Build. Mater. 398, 132375 https://doi.org/10.1016/j.conbuildmat.2023.132375.

Glossary

T: temperature field for cuboid sample geometry
T_N: temperature field inside the specimen
t: time
z: axial space coordinate; *x, y* transversal space coordinates
L_1: length of the sample on the left; L_2 length of the sample on the right (II + III); $L = (L_1 + L_2)/2$
2a: transversal size of the sample
q: Mean heat flow density at source
λ: Thermal conductivity
κ: Thermal diffusivity
α: Heat transfer coefficient for sample – ambient interface
c: specific heat capacity
$\Phi^*(u)$: the complementary error function
μ_n: the roots of the equation $\beta \cos \mu - \mu \sin \mu = 0$
R: the electrical resistance of the heat source [Ωm^{-2}]
t_0: the width of the current pulse
ρ: the sample's density under room conditions
I: the heating current passing the plane heat source
h: the width of the sample, *e* Euler's number
T_m: the maximum of the thermal response measured at the time t_m